Global and Planetary Change 161 (2018) 108–120

Contents lists available at ScienceDirect

Global and Planetary Change

journal homepage: www.elsevier.com/locate/gloplacha

Miocene vegetation shift and climate change: Evidence from the Siwalik of Nepal

Gaurav Srivastava[a], Khum N. Paudayal[b], Torsten Utescher[c,d], R.C. Mehrotra[a,*]

[a] Birbal Sahni Institute of Palaeosciences, 53 University Road, Lucknow 226 007, India
[b] Central Department of Geology, Tribhuvan University, Kirtipur, Kathmandu, Nepal
[c] Steinmann Institute, University of Bonn, Bonn, Germany
[d] Senckenberg Research Institute, Frankfurt am Main, Germany

ARTICLE INFO

Editor: Zhengtang Guo

Keywords:
C_4 plants
Churia Group
Fossils
Himalaya
Indian summer monsoon
Surai Khola

ABSTRACT

We reconstruct climate and vegetation applying the Coexistence Approach (CA) methodology on two palaeofloras recovered from the Lower (middle Miocene; ~13–11 Ma) and Middle Siwalik (late Miocene; 9.5–6.8 Ma) sediments of Surai Khola section, Nepal. The reconstructed mean annual temperature (MAT) and cold month mean temperature (CMT) show an increasing trend, while warm month mean temperature (WMT) remains nearly the same during the period. The reconstructed precipitation data indicates that the summer monsoon precipitation was nearly the same during the middle and late Miocene, while the winter season precipitation significantly decreased in the late Miocene. The overall precipitation infers increased rainfall seasonality during the late Miocene. The vegetation during the middle Miocene was dominated by wet evergreen taxa, whereas deciduous ones increased significantly during the late Miocene.

The reconstructed climate data indicates that high temperature and significantly low precipitation during the winter season (dry season) in the late Miocene might have enhanced forest fire which favoured the expansion of C_4 plants over C_3 plants during the period. This idea gets further support not only from a recent forest fire in northern India that was caused by the weakening of winter precipitation, but also from the burnt wood recovered from the late Miocene Siwalik sediments of northern India.

1. Introduction

The collision of the Indian plate with the Eurasian plate resulted in the formation of the Himalaya-Tibet Plateau during the Neogene which not only influenced the regional climate of Asia, but also the global climate (Wang et al., 2014). Regionally, the Himalaya-Tibet Plateau is considered to directly or indirectly control the strength and pattern of the Asian Monsoon System (ASM) (Molnar et al., 2010), though mechanisms involved remain controversial (Boos and Kuang, 2010, 2013; Zhang et al., 2015). The ASM consists of two sub-systems, namely the Indian and the East Asian Monsoon which are characterized by seasonal reversal of winds. The Indian summer monsoon (ISM) or Southwest monsoon (SWM) or South Asia summer monsoon (SASM) is tropical, while the East Asian monsoon (EAM) is extra-tropical in nature. The dynamics of both sub-systems are linked with the uplifting of the Himalaya (Raymo and Ruddiman, 1992; Guo et al., 2002) and the Tibetan Plateau (Molnar et al., 1993; Molnar et al., 2010). In the northern part of the Indian subcontinent the ISM is the major source of precipitation and during the winter season the area also receives rainfall from the Westerlies (Dimri et al., 2015). The Asian climate has been influenced by Westerlies since the Eocene (Caves et al., 2015) and has more impact on western and central Himalaya in comparison to eastern Himalaya. The south Asian climate is influenced by two types of circulation system: the ISM and the EAM, particularly the Westerlies (Dimri et al., 2015) (Fig. 1).

The orogenic movement of Himalaya during the Miocene not only shaped the ISM (Ding et al., 2017) but also boosted the evolution, diversification and migration of biota in the region (Mehrotra et al., 2005; Srivastava and Mehrotra, 2010; Che et al., 2010; Wang et al., 2012; Zhao et al., 2016; Liu et al., 2017). The increased rainfall seasonality in South Asia is due to the orogenic movement of Himalaya during the Miocene (Ding et al., 2017) which modified the vegetation of this area (Mehrotra et al., 2005). Moreover, the joining of the Indian and Eurasian plates during the early Miocene facilitated the migration of plant taxa from Southeast Asia to the Indian subcontinent and vice-versa, and diversified the floristic composition (Srivastava and Mehrotra, 2010; Mehrotra et al., 2014; Srivastava et al., 2014). Based on a phylogenetic study Klaus et al. (2015) recently suggested a sharp increase in the number of dispersal

* Corresponding author.
E-mail address: rcmehrotra@yahoo.com (R.C. Mehrotra).

https://doi.org/10.1016/j.gloplacha.2017.12.001
Received 15 June 2017; Received in revised form 28 November 2017; Accepted 2 December 2017
Available online 06 December 2017
0921-8181/

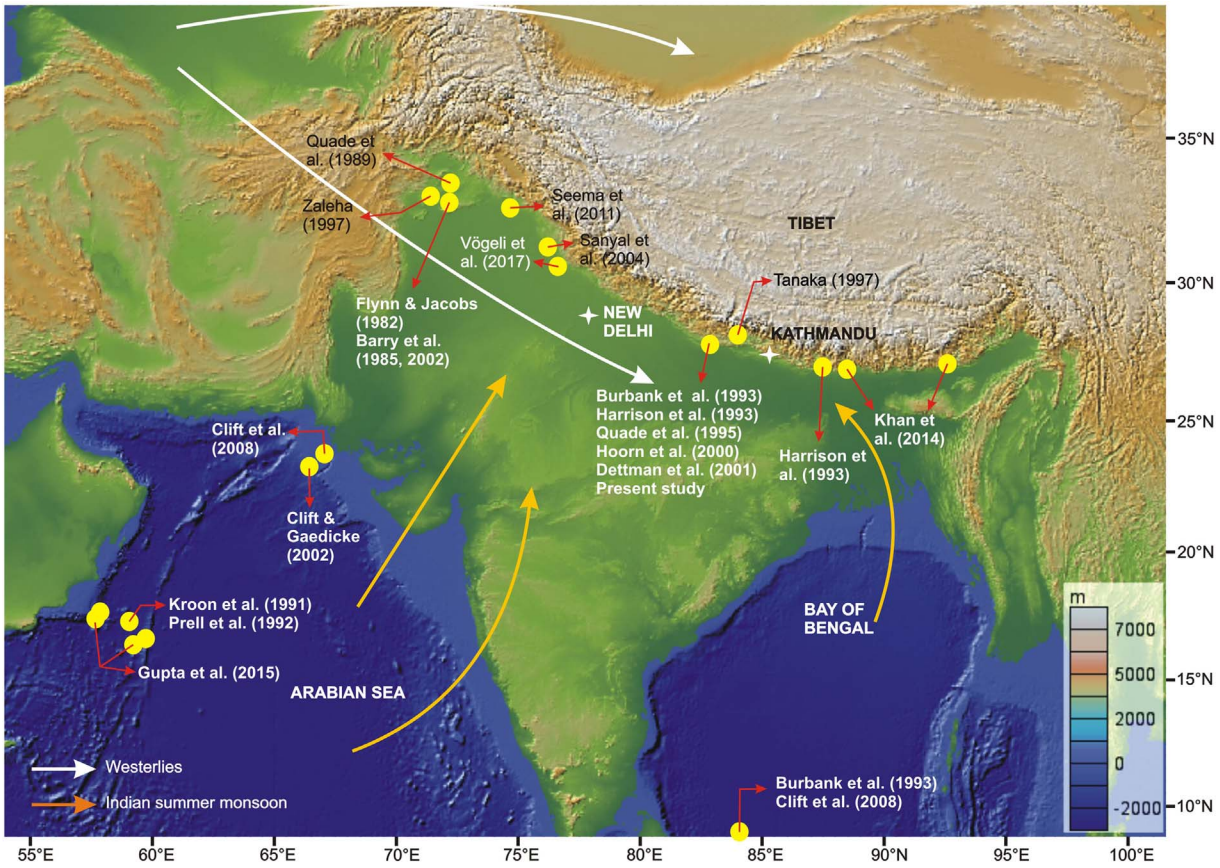

Fig. 1. Physiographic map showing the fossil locality presently studied and previous evidence of Miocene climate change in South Asia. (Modified after Allen and Armstrong, 2012) (Map source: http://www.geomapapp.org).

events (DEs) for biotic (flora and fauna) exchange from mainland Asia into the Indian subcontinent since 21 Ma, peaking at 15 Ma. From 14 Ma onwards, DE decreased again, due to increased seasonality of rainfall over northern India which resulted in an expansion of grasses in the late Miocene (Sanyal et al., 2010; Singh et al., 2011).

Extensive work has been done using different proxies to reconstruct the evolution of the ISM during the Miocene, and most reconstructed data point to an increase in precipitation seasonality during 10–6 Ma (Allen and Armstrong, 2012 and references therein) (Fig. 1; Table 1). Recently, Betzler et al. (2016) found evidence of strong ISM winds from the sediments of the Inner Sea of the Maldives at 12.9 Ma, albeit previous reconstructions from the Bengal and Indus fans (Clift et al., 2008; Clift and Gaedicke, 2002), as well as the Oman margin and Owen Ridge, western Arabian Sea (Gupta et al., 2015), support a weaker than present proto-monsoon between 25 and 12.9 Ma. The palaeoclimate reconstruction based on leaf architecture from the Siwalik of northeast India indicates a weak monsoon during the Miocene (Khan et al., 2014) (Table 1).

It has been suggested that increase in seasonality of rainfall/aridity during the late Miocene led to the expansion of C_4 plants in the western and central Himalayan Foreland Basin (Singh et al., 2011 and references therein). Moreover, Wu et al. (2014), by an inverse vegetation modeling study in the Siwalik of the Surai Khola section, inferred that the expansion of the C_4 plants during the late Miocene might have been triggered by regional aridification and temperature increase. A recent study based on carbon and oxygen isotopes from the Siwalik sediments of eastern and western Himalayan region suggested that the vegetation shift from C_3 to C_4 occurred only in the western region during the late Miocene and the most probable reason for this vegetation shift was due to the weakening of winter precipitation caused by the Westerlies (Vögeli et al., 2017).

Land plants, particularly mega-remains, are considered a reliable proxy for the quantitative reconstruction of palaeoclimate because they are directly controlled by their corresponding climate and therefore are preferably used to appraise the capabilities of global climate models (Spicer et al., 2008). A well-preserved plant megafossil record, in contrast to pollen, always ensures that the transportation of the components was not more than a few hundred metres so that the palaeoclimate reconstruction could reflect a past local climate (Spicer, 1981; Ferguson, 1985; Spicer and Wolfe, 1987).

In the present communication, we use plant megafossils to quantitatively reconstruct middle and late Miocene climate and vegetation. The plant megafossils were recovered from the well dated Surai Khola section of Surai Khola, Nepal. This section bears a continuous sequence of Lower, Middle, and Upper Siwalik sediments (Figs. 2, 3). Based on our climate and vegetation reconstruction the following questions are assessed:

1. How did climate change in the study area throughout the middle and late Miocene?
2. Are climate and floristic diversity linked to each other?
3. What factors were responsible for the expansion of C_4 plants?

2. Study area

2.1. A brief review of the Surai Khola section of western Nepal

Due to the uplift of the Himalaya fluvial muds, sands, and gravel have been deposited since the middle Miocene between the Lesser Himalaya (in the north) and the Gangetic Plains (in the south) attaining a thickness of ca. 6 km. These deposited sediments, in a coarsening-upward succession, are denoted Siwalik Group or Churia Group in

Table 1
Miocene climate change in south Asia.
(Modified after Allen and Armstrong, 2012).

Inferred climate change	Geological time (Ma)	Region	Evidence	Reference
Increased seasonality	7	Southeast Nepal	Changes in soil carbonate $\delta^{13}C$	Harrison et al. (1993)
Increased seasonality	7–6	Southeast Nepal	Changes in soil carbonate $\delta^{18}O$ and $\delta^{13}C$	Quade et al. (1995)
Increased seasonality	8	Northern Pakistan	Changes in soil carbonate $\delta^{18}O$ and $\delta^{13}C$	Quade et al. (1989)
Increased seasonality	10–6	Northern India	Changes in soil carbonate $\delta^{18}O$ and $\delta^{13}C$	Sanyal et al. (2004)
Increased seasonality with seasonal aridity	10.1–9	Northern Pakistan	Changes in fluvial sedimentology; vertebrate paleontology	Barry et al. (2002)
Unclear- reduced glaciations?	8	Bengal fan	Reduced sediment flux	Burbank et al. (1993)
Strong seasonality	15–9	Northern Pakistan	Variations in palaeosols	Zaleha (1997)
Increased aridity	7	Northern Pakistan	Vertebrate paleontology	Flynn and Jacobs (1982)
Increased aridity	7	Northern Pakistan	Vertebrate paleontology	Barry et al. (1985)
Increased aridity	7.5	Southeast Nepal	$\delta^{18}O$ trend in shells and mammal teeth	Dettman et al. (2001)
Increased aridity	8–6.5	Southeast Nepal	Vegetation change (based on pollen)	Hoorn et al. (2000)
Increased seasonality	10	Southeast Nepal	Changes in soil carbonate $\delta^{13}C$ and fluvial sediments	Tanaka (1997)
Summer monsoon wind	8	Arabian sea	Increase in *Globigerina bulloides*	Kroon et al. (1991)
Summer monsoon wind	8	Arabian sea	Increase in *Globigerina bulloides*	Prell et al. (1992)
Summer monsoon wind	12.9	Inner Sea of the Maldives	Geophysical and geochemical data	Betzler et al. (2016)
Summer monsoon wind	12.9	Western Arabian Sea	Increase in *Globigerina bulloides*, total organic carbon (TOC) and $\delta^{18}O$ and $\delta^{13}C$ of benthic foraminifer	Gupta et al. (2015)
Strong monsoon (increased precipitation)	16–11	Arabian Sea, Indus fan	High sediment flux	Clift and Gaedicke (2002)
Strong monsoon (increased precipitation)	16–11	Indus fan, Bengal fan	High sediment flux; chemical weathering	Clift et al. (2008)
Weak monsoon	16–5.3	Northeast India	Leaf fossils	Khan et al. (2014)

Nepal which is further sub-divided into three sub-groups, namely Lower, Middle, and Upper Siwalik (Valdiya, 2002). In west Nepal, along the Mahendra Highway and the Surai Khola river, a complete, undisturbed sequence of the Siwalik Group of ~5500 m consists of rocks of all three subgroups, the upper Lower Siwalik, Middle Siwalik and uppermost Upper Siwalik, whose strata strike WNW to ESE and dip 60°–80° to the north (Rösler and Appel, 1998; Corvinus and Rimal, 2001) (Fig. 2). The section is bounded by the Rangsing Khola Thrust (RKT) to the north and the Himalayan Frontal Thrust (HFT) to the south (Fig. 2). Above the RKT the Siwalik succession repeats and reaches up to Main Boundary Thrust (MBT). Corvinus and co-authors published extensive works on geology, lithostratigraphy, and paleontology of the Surai Khola area (Corvinus, 1988, 1990, 1993a, 1993b, 1994; Corvinus and Nanda, 1994; Corvinus and Schleich, 1994; Corvinus and Rimal, 2001). Moreover, several other workers conducted studies on the same section, including facies analysis, isotopes, magnetostratigraphy, palynology, and petrography (Appel et al., 1991; Rösler and Appel, 1998; Nakayama and Ulak, 1999; Hoorn et al., 2000; Ojha et al., 2009; Sanyal et al., 2005b; Baral et al., 2016).

Corvinus (1990) divided the entire Surai Khola section into five formations, namely Bankas (Lower Siwalik), Chor Khola (Middle Siwalik), Surai Khola (belonging mostly to the Middle Siwalik), Dobatta (= Pinjore), and Dhan Khola (= boulder conglomerate). The Bankas Formation mainly consists of mottled claystones and siltstones with distinct purple and red-brown colours and well-bedded sandstones. This formation represents the fluvial regime of a low energy environment and is composed of predominantly argillaceous sediments laid down in the quiet river, swamp and pool environments. The Chor Khola Formation follows the Bankas Formation and consists of alternations of mudstones, shales, and sandstones. The mudstones are grey and yellow coloured and intercalated with fine-grained sandstones increasingly frequent at the upper levels. The fossiliferous shales are interbedded between the mudstones and sandstones. The sediments of this formation represent channel and overbank deposits. The Chor Khola Formation is overlain by the Surai Khola Formation which consists of very coarse grained, multi-storey sandstones having a salt and pepper texture, deposited by a wide, braided river system. This formation shows increasing fluvial activity evidenced by the presence of large mud clasts in the sandstones pointing to high flood conditions, flushing overbank debris into the sand bars. The Dobatta Formation follows the Surai Khola Formation and shows evidence of a quieter fluvial regime. The discordant Dhan Khola Formation consists of conglomerates composed of pebble to cobble sized quartzite (Fig. 3) (Table 2). In general, the whole sequence represents the change from a lower energy fluvial environment to a very high energy fluvial system.

2.2. Brief description of rainfall patterns in the study area

At present, rainfall in the study area can be divided into four seasons: the pre-monsoon season envelops three months, March, April and May (MAM), the ISM covers four months, i.e. June, July, August, and September (JJAS), and the post-monsoon season consists of two months, namely October and November (ON). The dry season envelops three months, namely December, January, and February (DJF). The pre-monsoon season (MAM) is characterized by cyclonic storms. On the land, the weather is influenced by thunderstorms associated with rain. The ISM is the most prominent feature of the climate of the study area as the maximum rainfall is received only during this season (JJAS). Moreover, the area also receives rainfall during the winter season (DJF) from the Westerlies (Kansakar et al., 2004).

3. Materials and methods

3.1. Fossil flora and age of the Surai Khola section, Nepal

The flora lists selected for the present study refer to the megafossil records published by Awasthi and Prasad (1990), Prasad and Awasthi (1996), and Prasad and Pandey (2008). They have very carefully unearthed megafossils from the Bankas and Chor Khola formations of the Surai Khola section in western Nepal (Fig. 1; 27° 48′ 2.4″ N; 82° 54′ 2″ E). Magnetostratigraphic data available for the Surai Khola section show that the sediments of the Bankas Formation (Lower Siwalik) were deposited around ~13–11 Ma (late middle Miocene), while the sediments of the Chor Kola Formation (Middle Siwalik) were deposited between 9.5 and 6.8 Ma (late Miocene) (Sanyal et al., 2005a).

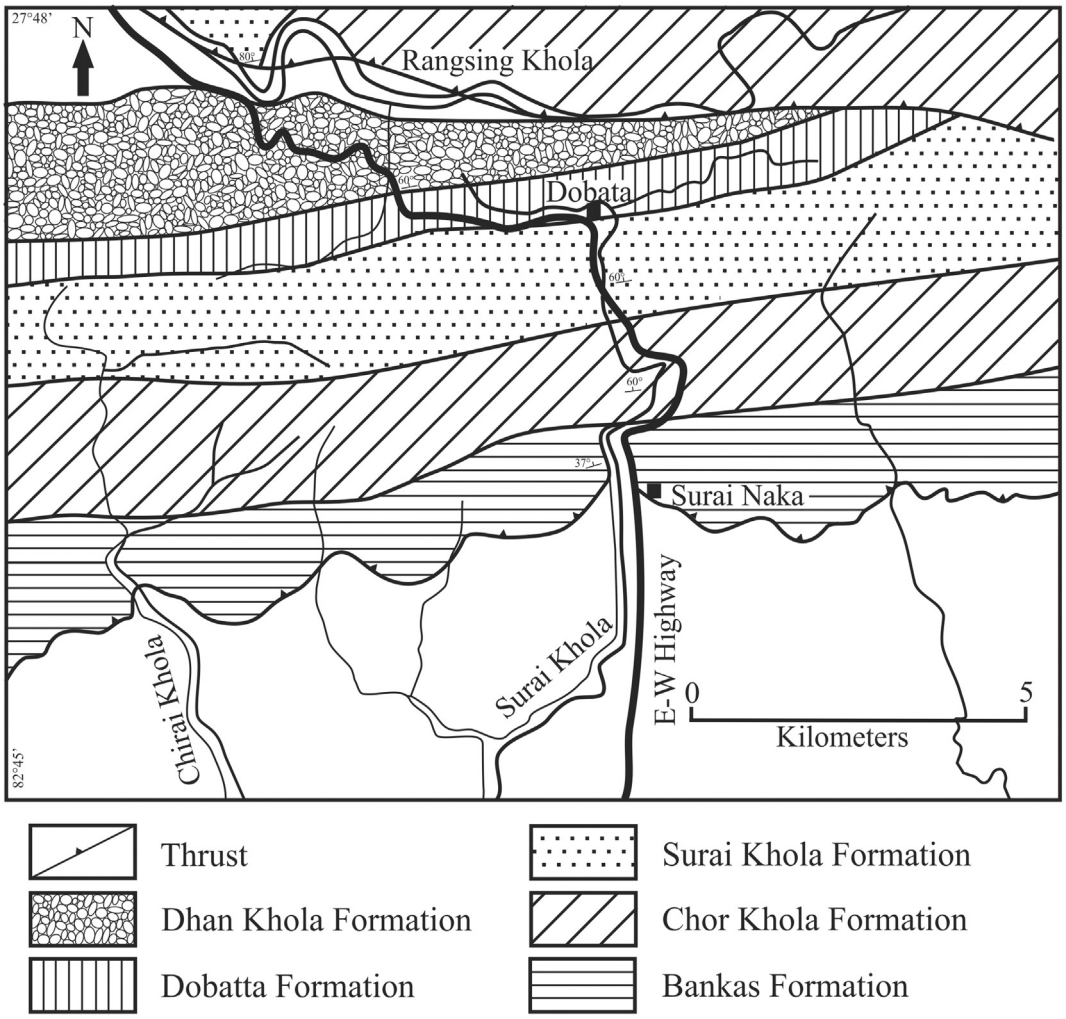

Fig. 2. Geological map of the Surai Khola area, Nepal.
(Modified after Corvinus and Rimal, 2001).

3.2. Methodology

For quantitative palaeoclimate reconstruction, we use the Coexistence Approach (CA). This technique can be applied on any fossil assemblage of leaves, fruits, wood, seeds and pollen (Mosbrugger and Utescher, 1997; Utescher et al., 2014). The CA entrusts that the fossil plants have a close affinity with their modern analogs and uses the climatic requirements of Nearest Living Relatives (NLRs) to infer the climatic conditions under which a fossil assemblage existed. Thus, the CA is most suitable to reconstruct Neogene to Quaternary conditions where in the majority of cases no significant change in environmental requirements of any taxon is expected (MacGinitie, 1941; Hickey, 1977; Chaloner and Creber, 1990; Mosbrugger, 1999). In the CA, first of all, the fossil taxa are identified to their modern counterparts i.e. NLRs. Then, the climatic tolerances of all NLR taxa known for a given fossil flora are obtained by listing the climatic conditions of the plant distribution area. After this, the "coexistence interval" (CI) is calculated for each climate variable that allows the majority of NLRs of a fossil flora to coexist. The resulting coexistence intervals are then considered as the most probable ranges of different palaeoclimate variables for a fossil flora. In the ideal case, there exists a single interval of a given climate variable within which all the NLRs (i.e. 100%) of a fossil flora can coexist. In various cases, climatic intervals do not overlap with the majority of ranges. Such taxa are denoted as outliers. The occurrence of outliers may have various causes such as specific taphonomic conditions, wrong identifications of NLRs, and inaccurate information of their climatic requirements. The exclusion of outliers may minimize the effect of anomalous environmental signals. For more details, the reader is referred to the original papers (Mosbrugger and Utescher, 1997; Utescher et al., 2014). The CA relies only on the presence/absence of the taxa and not on their abundance and is thus independent of the sampling size and some taphonomic filtering. The reliability of this technique has been checked by other techniques such as Climate Leaf Analysis Multivariate Program (CLAMP) and Leaf Margin Analysis (LMA) on the same fossil flora showing consistent results (Liang et al., 2003; Uhl et al., 2007; Xing et al., 2012; Bondarenko et al., 2013). CA based results also complement palaeoclimate data from marine archives and palaeovegetational reconstructions (Mosbrugger et al., 2005; Utescher et al., 2015; Srivastava et al., 2016). Thorough studies were made in China aiming at quantitative estimations of palaeoclimate and EAM intensity during the Cenozoic by using the technique CA on micro and mega flora (Xia et al., 2009; Jacques et al., 2011; Liu et al., 2011; Qin et al., 2011; Quan et al., 2011, 2012; Yao et al., 2011; Xing et al., 2012; Su et al., 2013; Wang et al., 2013; Huang et al., 2015; Li et al., 2015; Liu and Quan, 2016).

The climatic parameters discussed here are mean annual temperature (MAT), mean temperature of the warmest month (WMT), mean temperature of the coldest month (CMT), mean annual precipitation (MAP), mean precipitation of the wettest months (MPwet), mean precipitation of the warmest months (MPwarm), and mean precipitation of the driest months (MPdry). Moreover, the mean annual range of temperature (MART) can be determined as the difference between summer

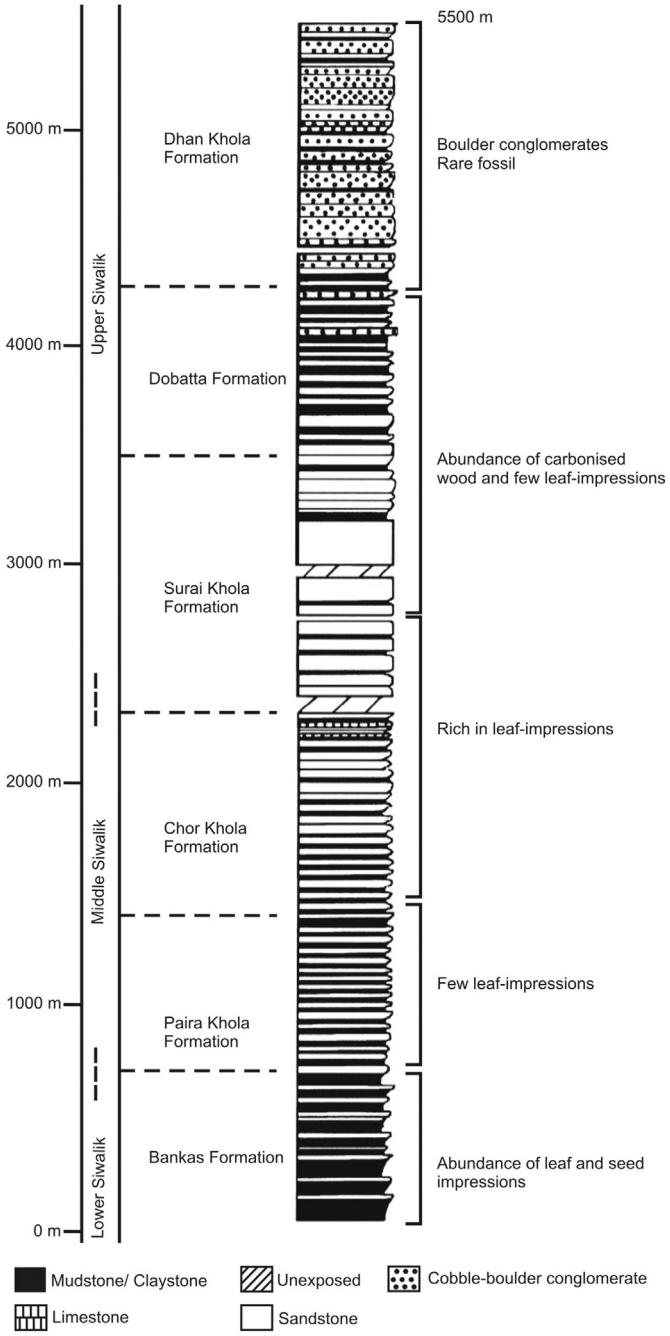

Fig. 3. Lithology of the Surai Khola section of Nepal showing different formations (Redrawn after Corvinus and Rimal, 2001).

and winter temperatures (MART = WMT-CMT), while the mean annual range of precipitation (MARP) is calculated as the difference between wettest and driest month precipitation (MARP = MPWET-MPDRY). The climatic tolerances of all NLRs known for the fossil floras were taken from the PALAEOFLORA database (Utescher and Mosbrugger, 2015).

4. Results

4.1. Palaeofloristic analysis of the Bankas (middle Miocene) and Chor Khola formations (late Miocene)

The palaeofloristic analysis of the middle Miocene and late Miocene assemblages indicates that in the middle Miocene Fabaceae was the most dominant family, followed by Euphorbiaceae and Rubiaceae and then by Lauraceae and Meliaceae while the minor parts of the assemblages are represented by taxa belonging to Ancistrocladaceae, Anonaceae, Clusiaceae, Connaraceae, Flacourtiaceae, Menispermaceae, Sapindaceae, and Sterculiaceae families (Fig. 4A). Moreover, in the late Miocene two families, namely Dipterocarpaceae and Fabaceae were equally dominant, followed by Euphorbiaceae, Anonaceae, Sapindaceae and Sterculiaceae families, while rest of the assemblage is represented by Anacardiaceae, Apocynaceae, Calopyllaceae, Clusiaceae, Ctenolophonaceae, Flacourtiaceae, Lauraceae, Lythraceae, Myrtaceae, Ochnaceae, Poaceae, Rubiaceae, and Rutaceae (Fig. 4B).

During the middle and late Miocene several families such as Anonaceae, Clusiaceae, Euphorbiaceae, Fabaceae, Flacourtiaceae, Lauraceae, and Rubiaceae were common, though they differ in their species diversity (Fig.4A, B). In the middle Miocene, the most diverse families were Fabaceae, Euphorbiaceae, Rubiaceae, Lauraceae and Meliaceae, while in the late Miocene families such as Dipterocarpaceae, Fabaceae, Euphorbiaceae, Anonaceae, Sapindaceae and Sterculiaceae were more common (Fig.4A, B). Many families which are not observed in the middle Miocene, were present in the late Miocene, e.g. Anacardiaceae, Apocynaceae, Calophyllaceae, Ctenolophriaceae, Myrtaceae, Ochnaceae, Poaceae, and Rutaceae (Fig. 4A, B). Based on the fossil records from the middle and late Miocene of Surai Khola we infer that the late Miocene flora was more diverse than the middle Miocene flora (Fig. 4A, B).

The study of the floristic assemblage from the middle Miocene indicates that 62.5% taxa belong to the wet evergreen forest, 25% taxa are part of wet evergreen and moist deciduous forests, while 8.33% taxa are related to the moist deciduous forest and only 4.17% taxa are associated with the littoral and swamp forest (Fig. 4C). In the late Miocene flora 38.7% taxa belong to both wet evergreen and wet evergreen to moist deciduous forests, while only 22.6% taxa correspond to the moist deciduous forest (Fig. 4D).

4.2. Temperature and rainfall reconstruction of the Bankas (middle Miocene) and Chor Khola formations (late Miocene)

The CA reconstruction for the Bankas Formation can be based on a total of 18 NLR taxa known for the leaves (Fig. S1) occurring in the

Table 2
Lithology of the Surai Khola section, Nepal.
(After Corvinus and Rimal, 2001).

Local formation	Lithology
DhanKhola (1500 m)	Consolidated to un-consolidated cobble to boulder conglomerates, subordinate yellow, soft sandstones and siltstones.
Dobatta (550 m)	Alternation of yellow-brown and grey clays + mudstones with soft micaceous medium to coarse grained sandstones.
SuraiKhola (1150 m)	Massive grey to beige, micaceous, medium to coarse grained sandstone with few intercalations of dark grey clays.
ChorKhola (Upper member) (850 m)	Alternations of calcareous grey-greenish to buff fine to medium grained sandstones with mottled siltstones and claystones. Sandstone percentage increasing in younger beds. First appearance of salt and pepper sandstone bed, limestone beds in uppermost part.
ChorKhola (Lower member) (950 m)	Alternations of grey to greenish, calcareous, fine grained sandstones with mottled variegated mudstones/claystones.
Bankas (600 m)	Variegated, mottled claystones and mudstones with subordinate grey, calcareous fine-grained sandstone.

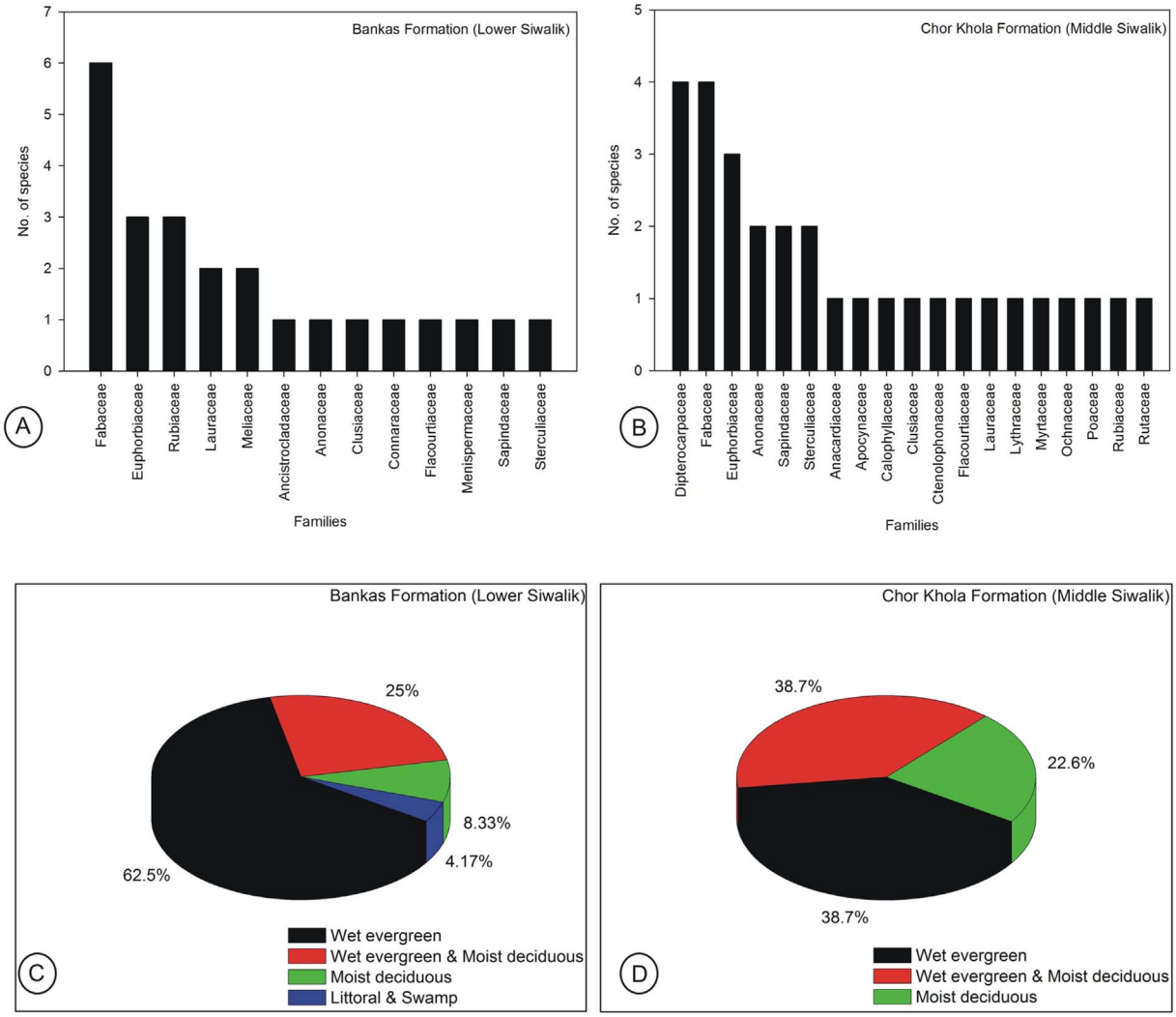

Fig. 4. Floristic diversity and forests types. (A) and (B) floristic diversity during the Lower Siwalik (middle Miocene) and Middle Siwalik (late Miocene); (C) and (D) forest types during the Lower Siwalik (middle Miocene) and Middle Siwalik (late Miocene).

sediments (Table 3; Fig. 5). A list of all plant fossils, their Nearest Living Relatives (NLRs), and abbreviations used in Fig. 5 are provided in Table 3.

The reconstructed temperature CIs obtained from the above flora are: 21.1–25.4 °C for MAT (average ~23.3 °C), 27.5–28.1 °C for WMT (average ~27.8 °C), 20.6–24.3 °C for CMT (average ~22.4 °C), and MART ~5.4 °C (calculated using averages). The reconstructed CIs of the precipitation are: 1748–2869 mm for MAP (average ~2308.5 mm), 300–329 mm for MPwet (average ~314.5 mm), 46–135 mm for MPdry (average ~90.5 mm), 128–221 mm for MPwarm (average ~174.5), and ~224 mm for MARP (calculated using averages). The results of the CIs are given in Tables 4 and 5. As 100% of the NLR taxa coexist in the resulting CIs, results are considered highly significant. The CA reconstruction for the Chor Khola Formation can be based on a total of 28 NLR taxa identified from the fossil leaf record (Fig. S2) (Table 3; Fig. 6). A list of all the plant fossils, their Nearest Living Relatives (NLRs) and abbreviations used in Fig. 6 are provided in Table 3.

The reconstructed temperature CIs of the above flora are: 26–27 °C for MAT (average ~26.5 °C), 26.7–27.8 °C for WMT (average ~27.3 °C), 24.3–24.7 °C for CMT (average ~24.5 °C), and MART ~2.8 °C (calculated using averages). Precipitation reconstruction indicates CIs of 2592–3151 mm for MAP (average ~2871.5 mm), 225–389 mm for MPwet (average ~307 mm), 8–59 mm for MPdry (average ~33.5 mm), 206–221 mm for MPwarm (average ~213.5 mm), and ~273.5 mm for MARP (calculated using averages). Climatic ranges of all the taxa included as NLRs overlap in the CIs except for MPwet, where *Ctenolophon* forms a wet outlier.

5. Discussion

5.1. Change in forest types, temperature, precipitation, and monsoonal pattern during the Bankas (middle Miocene) and Chor Khola (late Miocene) formations

It is interesting to note that the middle Miocene forests were different from the late Miocene forests of Surai Khola, Nepal. The dominance of wet evergreen taxa over the moist deciduous ones and the presence of littoral and swamp taxa in the middle Miocene floral assemblage indicate high rainfall with low seasonality in precipitation during the deposition of the sediments. However, in the late Miocene floral assemblage the percentage of moist deciduous taxa increased significantly, moreover, no littoral and swamp taxa are observed thus indicating increased seasonality in rainfall (Fig. 4C, D). Similarly, pollen data from Surai Khola also suggest the existence of wet evergreen forest during the middle Miocene which was replaced by moist deciduous forest in the late Miocene (Sarkar, 1990).

The reconstructed temperature data indicate that MAT and CMT were lower by 3.2 °C and 2.1 °C respectively in the middle Miocene

Table 3
Fossil plants and their NLRs from the Surai Khola section, Nepal.

Fossil taxa	NLRs	Abbreviations
LOWER SIWALIK (Bankas formation)		
Albizia microfolia Prasad & Awasthi	*Albizia* sp.	*Albizi* sp.
Cinnamomum nepalensis Prasad & Pandey	*Cinnamomum* sp.	*Cinnam* sp.
Cocculus miotrilobus Prasad & Pandey	*Cocculus* sp.	*Coccul* sp.
Cynometra palaeoiripa Prasad et al.	*Cynometra* sp.	*Cynome* sp.
Cleistanthus suraikholaensis Prasad & Awasthi	Euphorbiaceae	Euphorb
Millettia churiensis Prasad & Awasthi	Fabaceae	Fabacea
Ficus raptiensis Prasad & Awasthi	*Ficus* sp.	*Ficus* sp.
Koompassia suraikholaensis Prasad & Awasthi	*Koompassia* sp.	*Koompa* sp.
Machilus miocenica Prasad	*Machilus* sp.	*Machil* sp.
Mallotus venkatachalai (Prasad) Prasad & Awasthi	*Mallotus* sp.	*Mallot* sp.
Chisocheton suraikholaensis Prasad & Pandey	Meliaceae	Meliace
Mesua tertiara Lakhanpal	*Mesua* sp.	*Mesua* sp.
Mucuna miogigantea Prasad & Pandey	*Mucuna* sp.	*Mucuna* sp.
Olax bankasii Prasad & Pandey	Olacaceae	Olacaceae
Phyllanthus palaeoreticulatus Prasad & Awasthi	*Phyllanthus* sp.	*Phylla* sp.
Polyalthia palaeosimiarum Awasthi & Prasad	*Polyalthia* sp.	*Polyal* sp.
Xerospermum mioglabratum Prasad & Pandey	Sapindaceae	Sapinda
Sterculia mioensifolia Prasad & Pandey	*Sterculia* sp.	*Stercu* sp.
MIDDLE SIWALIK (Chor Khola formation)		
Actinodaphne palaeoangustifolia Prasad & Pandey	*Actinodaphne* sp.	*Actinod*
Albizia siwalika Prasad	*Albizia*	*Albizi*
Goniothalamus chorkholaensis Prasad & Awasthi	Anonaceae	Anonace
Chonemorpha miocenica Prasad & Awasthi	Apocynaceae	Apocyna
Bridelia mioretusa Prasad & Pandey	*Bridelia* sp.	*Brideli*
Calophyllum suraikholaensis Awasthi & Prasad	*Calophyllum* sp.	*Calophy*
Chukrasia miocenica Prasad & Awasthi	*Chukrasia* sp.	*Chukras*
Ctenolophon chorkholaensis Prasad & Pandey	*Ctenolophon* sp.	*Ctenolo*
Diospyros miocenicus Prasad & Awasthi	*Diospyros* sp.	*Diospyr*
Dipterocarpus siwalicus Awasthi & Prasad	Dipterocarpaceae	Diptero
Dipterocarpus suraikholaensis Prasad & Pandey	*Dipterocarpus* sp.	*Dipter* sp.
Excoecaria palaeocrenulata Awasthi & Prasad	Euphorbiaceae	Euphorb
Millettia koilabasensis Prasad	Fabaceae	Fabacea
Garcinia corvinusiana Prasad & Pandey	*Garcinia* sp.	*Garcini*
Duabanga siwalika Prasad & Pandey	Lythraceae	Lythrac
Mallotus kalimpongensis Antal & Awasthi	*Mallotus* sp.	*Mallotu*
Stigmaphyllon chorkholaensis Prasad & Pandey	Malpighiaceae	Malpigh
Mangifera suraikholaensis Prasad & Pandey	*Mangifera* sp.	*Mangif* sp.
Dysoxylum raptiensis Prasad & Awasthi	Meliaceae	Meliace
Artocarpus nepalensis Prasad & Awasthi	Moraceae	Moracea
Murraya khariensis Prasad & Awasthi	*Murraya* sp.	*Murraya*
Myrsine precapitellata Prasad & Pandey	*Myrsine* sp.	*Myrsine*
Ochna siwalika Prasad & Pandey	Ochnaceae	Ochnace
Harpullia siwalica Prasad & Awasthi	Sapindaceae	Sapinda
Shorea palaeostellata Prasad & Pandey	*Shorea* sp.	*Shorea*
Sterculia premontana Prasad & Pandey	*Sterculia* sp.	*Stercul*
Syzygium palaeocumini Prasad & Awasthi	*Syzygium* sp.	*Syzygiu*
Zanthoxylum siwalicum Prasad & Awasthi	*Zanthoxylum* sp.	*Zanthox*

compared to the late Miocene as far as the means of their CIs are concerned, while the WMT was nearly the same. The reconstructed MART indicates that the seasonality in temperature was more pronounced in the middle Miocene than the late Miocene. In general, the overall reconstructed temperature data indicate that the rise in MAT might be due to temperature rise in the cooler part of the year, while the warm season remained at the same level from the middle to late Miocene (Fig. 7A).

Our temperature reconstruction is supported by a modeling study on the Himalayan foreland basin (Wu et al., 2014). Wu et al. (2014) suggested an overall increasing trend in MAT in the Himalayan Foreland Basin during the Neogene as is evident from our results. Moreover, our reconstruction resolves seasonality of temperature indicating that the increase in MAT is due to temperature increase in the cooler part of the year (Table 4).

The reconstructed precipitation data indicate that MAP was significantly lower in the middle Miocene than the late Miocene as far as the means of CIs are taken into consideration (Table 5). The precipitation of the warmest month (MPwarm) shows an increasing trend (Table 5), while precipitation of the wettest months (MPwet) remains nearly at the same level (Fig. 7B), however, precipitation of the driest months (MPdry) was higher in the middle Miocene when compared to the late Miocene (Fig. 7B). In general, the reconstructed precipitation data indicate that during the middle Miocene the rainfall pattern was more equable, while in the late Miocene rainfall had become more seasonal (Fig. 7B) (Table 5).

The ISM is characterized by a seasonal reversal of surface wind, forced by the thermal gradient between the continental area and the Indian Ocean, which is mainly governed by solar radiation. The reconstructed precipitation data suggest that the rainfall during the summer monsoon season (JJAS) was the same during the middle and late Miocene. Our evidence for a strong summer monsoon during the middle Miocene coincides with previous reconstructions based on high sediment flux and chemical weathering from the Arabian Sea, Indus and Bengal fans (Clift and Gaedicke, 2002; Clift et al., 2008), increase in *Globigerina bulloides*, total organic carbon and oxygen and carbon isotopes of benthic foraminifera from the western Arabian Sea (Gupta et al., 2015) and geophysical and geochemical data from the Inner Sea of Maldives (Betzler et al., 2016) (Table 4; Fig. 7).

At present, rainfall during the winter season (DJF) in the northern part of the Indian Subcontinent is brought by the Westerlies, and because of them, the Himalaya receives immense amounts of snow during the winter season (Dimri et al., 2015). When assuming that the reconstructed MPdry expresses rainfall in the winter season (DJF), these rates were higher in the middle Miocene, but significantly lower in the late Miocene (Fig. 7B; Table 5). Thus our results imply that the summer monsoon rainfall remained at the same level, while the winter rainfall decreased from the middle to late Miocene resulting in an increased seasonality in precipitation during the late Miocene. Our MPdry (winter precipitation) reconstruction for the middle and late Miocene gets strong support from a recent Miocene climate reconstruction based on isotopic data from the Siwalik of the western Himalayan region (Vögeli et al., 2017).

5.2. Were floristic diversity and climate interlinked during the deposition of the Bankas (middle Miocene) and Chor Khola (late Miocene) formations?

In Section 5.1 we have shown that during the middle Miocene the flora was dominated by wet evergreen taxa while in the late Miocene, the diversity of deciduous taxa increased significantly (Fig. 4C, D). Moreover, our results indicate that during the middle Miocene precipitation was more equable, whereas it became more seasonal in the late Miocene (Fig. 7B). This may explain why the vegetation became dominantly deciduous during the late Miocene (Fig. 4C, D). The absence of littoral and swamp taxa in the late Miocene flora is in line with the inferred seasonally dry condition. Thus, our data imply that the rainfall pattern, floral assemblage, and floristic diversity were strongly interrelated throughout the studied time-span. Moreover, the role of fire during the late Miocene (explained in Section 5.3) cannot be ignored in enhancing floristic diversity because it delays competitive exclusion, enhanced landscape heterogeneity and generated new ecological niches (Pausas and Ribeiro, 2017).

5.3. Possible factors responsible for the expansion of C_4 plants during Middle Siwalik

C_3 plants are those in which the first stable product formed after carboxylation is three-carbon sugar (glyceraldehydes 3-phosphate), while in C_4 plants the first stable products are 4-carbon acids (malate and aspartate) (Taiz and Zeiger, 2002). Physiologically, C_4 plants are more efficient than C_3 plants under conditions of drought, high

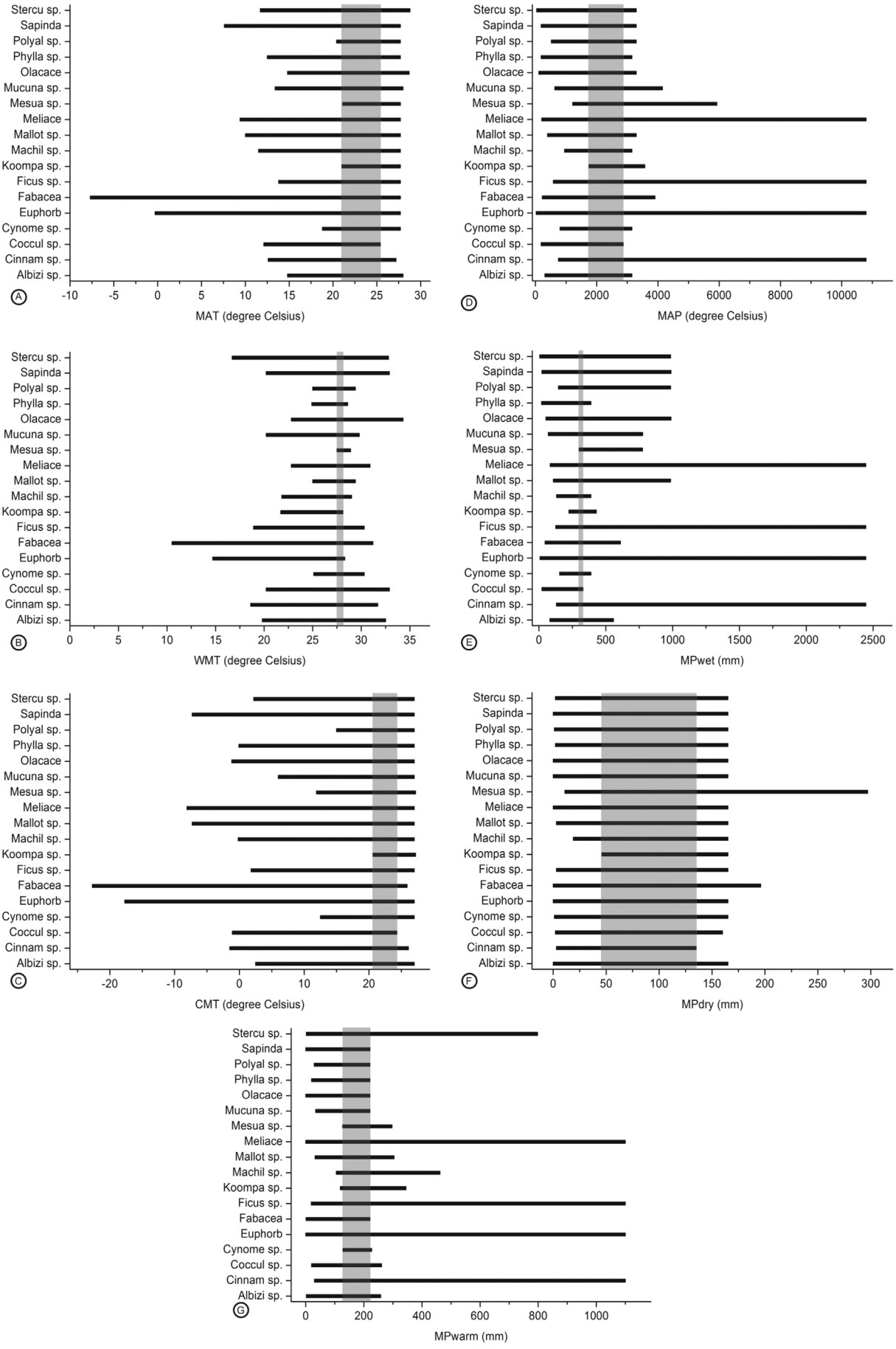

(caption on next page)

Fig. 5. Climatic ranges of the NLRs identified for the palaeoflora of the Lower Siwalik (Bankas Formation). Grey shaded areas: Coexistence Intervals (CIs) (A) mean annual temperature (MAT); (B) warm month mean temperature (WMT); (C) cold month mean temperature (CMT); (D) mean annual precipitation (MAP); (E) mean precipitation of the wettest month (MPwet); (F) mean precipitation of the driest month (MPdry); (G) mean precipitation of the warmest month (MPwarm).

Table 4
Border and centre values of coexistence intervals for temperature (LB = lower borders of coexistence interval, UB = upper borders of coexistence intervals, CV = centre values, MC = modern climate, RC = reconstructed climate).

Formations	Latitude; Longitude (Altitude)	MAT (°C)				WMT (°C)				CMT (°C)				MART (°C)	
		MC	LB	CV	UB	MC	LB	CV	UB	MC	LB	CV	UB	MC	RC
Bankas	27°48′2.4″ 82°54′2″ (705 m a.s.l.)	25.6	21.1	23.3	25.4	27.67	27.5	27.8	28.1	15.87	20.6	22.4	24.3	11.8	5.4
Chor Khola	27°48′2.4″ 82°54′2″ (705 m a.s.l.)	25.6	26	26.5	27	27.67	26.7	27.3	27.8	15.87	24.3	24.5	24.7	11.8	2.8

Table 5
Border and centre values of coexistence intervals for precipitation (LB = lower borders of coexistence interval, UB = upper borders of coexistence intervals, CV = centre values, MC = modern climate, RC = reconstructed climate).

Formations	MAP (mm)				MPwet (mm)				MPdry (mm)				MPwarm (mm)				MARP (mm)	
	MC	LB	CV	UB	MC	LB	CV	UB	MC	LB	CV	UB	MC	LB	CV	UB	MC	RC
Bankas	1146	1748	2308.5	2869	803	300	314.5	329	62	46	90.5	135	39	128	174.5	221	770	224
Chor Khola	1146	2592	2871.5	3151	803	225	307	329	62	8	33.5	59	39	206	213.5	221	770	273.5

temperatures, and CO_2 limitation, and this phenomenon allows for niche broadening (Lundgren et al., 2016) and survival in a variety of habitats, from the tropics to the boreal zone, from desert to submerged conditions, open grasslands to forest understorey, and from nutrient-depleted to fertile soils (Christin and Osborne, 2014). The lowering of atmospheric carbon dioxide concentration started during the late Eocene and continued up to the earliest Miocene favoring the evolution of C_4 pathway of photosynthesis (Tipple and Pagani, 2007). Molecular studies place the origin of C_4 plants between 33 and 25 Ma (Gaut and Doebley, 1997; Bouchenak-Khelladi et al., 2009). To study the expansion of C_4 plants during the Miocene, various carbon isotopes from soils have been analysed from continental areas of Asia, Africa, North America, and South America indicating that the expansion of C_4 plants did not occur synchronously global (Quade et al., 1989, 1994; Cerling, 1992; Cerling and Quade, 1993; Cerling et al., 1993; Kingston et al., 1994; Latorre et al., 1997; Fox and Koch, 2003, 2004) or regional (Sanyal et al., 2010). Data available from the Siwaliks indicate that the C_4 plants expanded during the late Miocene (Singh et al., 2011 and references therein) (Table 6), and as the most plausible reason, the intensification of the monsoon in South Asia can be cited (Table 1). The greater adaptability of C_4 plants over C_3 plants, in a variety of environmental conditions ensures that several factors were responsible for the expansion C_4 plants during the late Miocene. Sage (2004) suggested that the unique adaptability of C_4 plants in varied environmental conditions refers to a specific adaptation that compensates for high rates of photorespiration and carbon deficiency. Any environmental factor which promotes photorespiration can favour the C_4 photosynthesis and hence C_4 plants. High temperature, aridity, salinity, and low CO_2 stimulate photorespiration (Sage, 2004). Moreover, forest fire during the dry season is another important factor which promotes C_4 plants (Knapp and Medina, 1999; Bond, 2008). C_4 plants also contribute in forest fire ecology suppressing the growth of woody flora and hence creating an open habitat (Bond et al., 2005; Bond, 2008). In the present South Asian monsoonal climate, the warm, moist growing season ensures high biomass production, and this primary productivity itself provides combustible fuels in the following dry season. Moreover, the season just after the fire favours the fast growing C_4 plants in comparison to the C_3 plants (Keeley and Rundel, 2005).

Our climate and vegetation reconstructions from the middle and late Miocene flora of the Siwalik suggest that during the middle Miocene the dominance of wet evergreen taxa might have suppressed the growth of C_4 plants, due to the closed canopy structure of the vegetation existing at that time (Wedin, 2004; Bond, 2008). However, during the late Miocene, deciduous taxa provided more open spaces for C_4 plants by shedding their leaves during the dry season. Moreover, the decrease in precipitation and inferred increase in temperature during the dry season in the late Miocene may have promoted forest fires and their frequency which supported the expansion of C_4 plants. This is in line with present observations made in northern India where decreasing winter precipitation leads to higher forest fire frequency (Sati and Juyal, 2016). Moreover, the presence of burnt wood in the late Miocene sediments of the Indian Siwalik confirms the occurrence of forest fire during this period (Sanyal et al., 2010).

6. Conclusions

We have reconstructed the climate evolution during the deposition of the Lower and Middle Siwalik sediments of Surai Khola, Nepal, using the Coexistence Approach and related impact on vegetation type and diversity. The reconstructed MAT and CMT show an increasing trend, while the WMT remains at the same level from the Lower to Middle Siwalik. The reconstructed precipitation data indicate that summer precipitation stayed at the same level from the Lower to Middle Siwalik, but winter precipitation decreases in the Middle Siwalik. The overall reconstructed precipitation indicates that from Lower to Middle Siwalik precipitation became more seasonal. The middle Miocene forest was dominated by the wet evergreen taxa, however, in the late Miocene, due to increased rainfall seasonality, the percentage of deciduous taxa increased significantly. The plant megafossil record from the Surai Khola section indicates that the late Miocene flora was more diverse than the middle Miocene flora.

The increase in temperature and decrease in precipitation during the winter season in the late Miocene probably caused an increase in forest fire frequency which contributed to the expansion of C_4 plants.

Supplementary data to this article can be found online at https://doi.org/10.1016/j.gloplacha.2017.12.001.

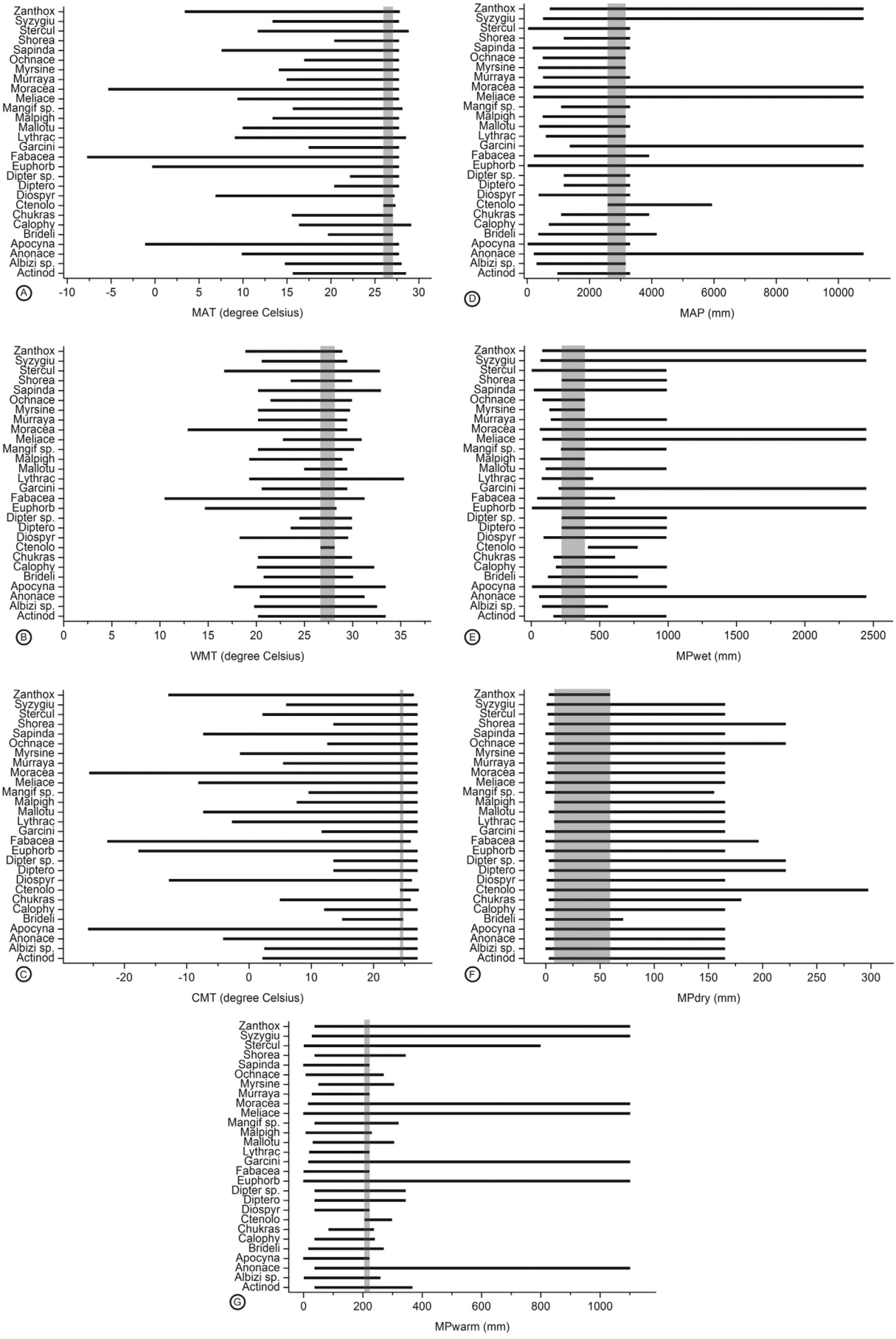

(caption on next page)

Fig. 6. Climatic ranges of the NLRs identified for the palaeoflora of the Middle Siwalik (Chor Khola Formation). Grey shaded areas: Coexistence Intervals (CIs) (A) mean annual temperature (MAT); (B) warm month mean temperature (WMT); (C) cold month mean temperature (CMT); (D) mean annual precipitation (MAP); (E) mean precipitation of the wettest month (MPwet); (F) mean precipitation of the driest month (MPdry); (G) mean precipitation of the warmest month (MPwarm).

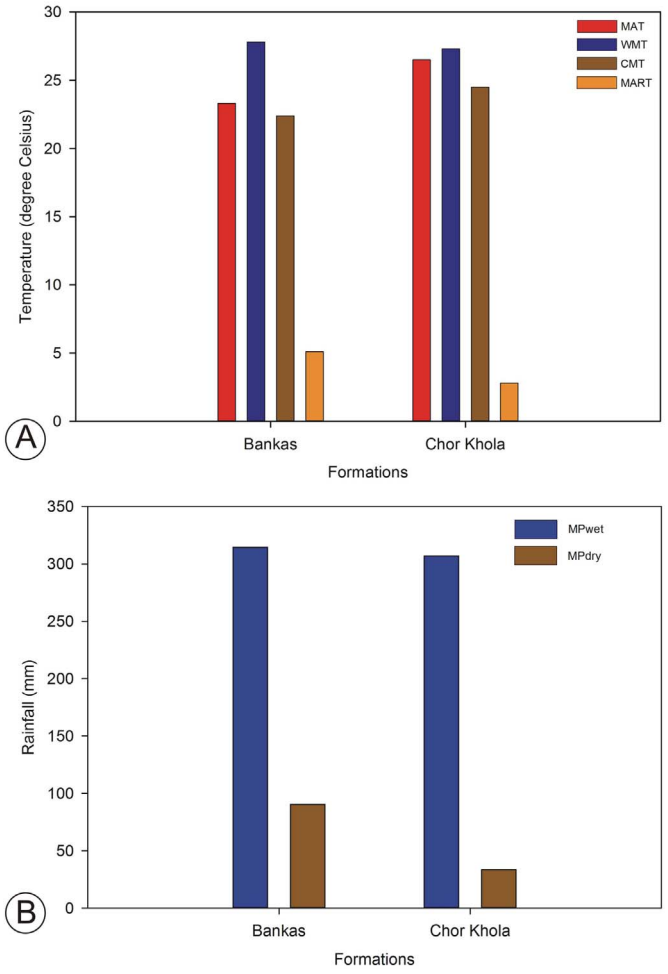

Fig. 7. Bar diagram showing temperature and rainfall. (A) temperature during the Bankas (middle Miocene) and Chor Khola (late Miocene) formations; (B) rainfall seasonality during Bankas (middle Miocene) and Chor Khola (late Miocene) formations.

Table 6
Ages proposed previously for Siwalik vegetation shift in the Indian subcontinent.

Locality	Vegetation shift towards C4 plants (Ma)	Reference
Siwalik of India	~6	Sanyal et al. (2004)
Siwalik of India	~7	Singh et al. (2011)
Siwalik of India	~7.3	Sanyal et al. (2005b)
Siwalik of India	~7	Vögeli et al. (2017)
Siwalik of Nepal	~8–~6.5	Hoorn et al. (2000)
Siwalik of Nepal	~7	Quade et al. (1995)
Siwalik of Nepal	~10	Tanaka (1997)
Siwalik of Pakistan	~7–7.4	Quade et al. (1989)
Siwalik of Pakistan	7.3	Quade et al. (1995)

Acknowledgements

GS and RCM are thankful to the Director, Birbal Sahni Institute of Palaeosciences, Lucknow for providing necessary facilities in carrying out the research work. KNP is grateful to the Head of Geology Department, Tribhuvan University, Nepal for constant encouragement. The authors express their gratitude to Prof. Zhengtang Guo and reviewers for their helpful suggestions. The present work is a contribution to NECLIME (Neogene Climate Evolution of Eurasia).

References

Allen, M.B., Armstrong, H.A., 2012. Reconciling the Intertropical Convergence Zone, Himalayan/Tibetan tectonics, and the onset of the Asian monsoon system. J. Asian Earth Sci. 44, 36–44.
Appel, E.W., Rösler, W., Corvinus, G., 1991. Magnetostratigraphy of the Miocene-Pleistocene Surai Khola Siwaliks in west Nepal. Geophys. J. Int. 105, 191–198.
Awasthi, N., Prasad, M., 1990. Siwalik plant fossils from Suria Khola area, western Nepal. Palaeobotanist 38, 298–318.
Baral, U., Lin, D., Chamlagain, D., 2016. Detrital zircon U–Pb geochronology of the Siwalik Group of the Nepal Himalaya: implications for provenance analysis. Int. J. Earth Sci. 105, 921–939.
Barry, J.C., Johnson, N.M., Raza, S.M., Jacobs, L.L., 1985. Neogene mammalian faunal change in southern Asia – correlations with climatic, tectonic and eustatic events. Geology 13, 637–640.
Barry, J.C., Morgan, M.L.E., Flynn, L.J., Pilbeam, D., Behrensmeyer, A.K., Raza, S.M., Khan, I.A., Badgley, C., Hicks, J., Kelley, J., 2002. Faunal and environmental change in the late Miocene Siwaliks of northern Pakistan. Paleobiology 28, 1–71.
Betzler, C., et al., 2016. The abrupt onset of the modern south Asian monsoon winds. Sci. Rep. 6, 29838.
Bond, W.J., 2008. What limits trees in C4 grasslands and savanna? Annu. Rev. Ecol. Syst. 39, 641–659.
Bond, W.J., Woodward, F.I., Midgley, G.F., 2005. The global distribution of ecosystems in a world without fire. New Phytol. 165, 525–538.
Bondarenko, O.V., Blochina, N.I., Utescher, T., 2013. Quantification of Calabrian climate in southern Primory'e, Far East of Russia—an integrative case study using multiple proxies. Palaeogeogr. Palaeoclimatol. Palaeoecol. 386, 445–458.
Boos, W.R., Kuang, Z., 2010. Dominant control of the south Asian monsoon by orographic insulation versus plateau heating. Nature 463, 218–222.
Boos, W.R., Kuang, Z., 2013. Sensitivity of the South Asian monsoon to elevated and non-elevated heating. Sci. Rep. 3, 1192.
Bouchenak-Khelladi, Y., Verboom, G.A., Hodkinson, T.R., Olivierfrancois, N.S., Chonghaile, G.N., Savolainen, V., 2009. The origins and diversification of C4 grasses and savanna adapted ungulates. Glob. Chang. Biol. 15, 2397–2417.
Burbank, D.W., Derry, L.A., France-Lanord, C., 1993. Reduced Himalayan sediment production 8 Myr ago despite an intensified monsoon. Nature 354, 48–50.
Caves, J.K., Winnick, M.J., Graham, S.A., Sjostrom, D.J., Mulch, A., Chamberlain, C.P., 2015. Role of the westerlies in Central Asia climate over the Cenozoic. Earth Planet. Sci. Lett. 428, 33–43.
Cerling, T.E., 1992. Development of grasslands and savannas in east Africa during the Neogene. Palaeogeogr. Palaeoclimatol. Palaeoecol. 97, 241–247.
Cerling, T.E., Quade, J., 1993. Stable carbon and oxygen isotopes in soil carbonates. In: McKenzie, J.A., Savin, S. (Eds.), Climate Change in Continental Isotopic Records: Geophys. Monogr. 78. pp. 217–231.
Cerling, T.E., Wang, Y., Quade, J., 1993. Expansion of C4 ecosystems as an indicator of global ecological change in the late Miocene. Nature 361, 344–345.
Chaloner, W.G., Creber, G.T., 1990. Do fossil plants give a climatic signal? J. Geol. Soc. Lond. 147, 343–350.
Che, J., Zhou, W.-W., Hu, J.-S., Yan, F., Papenfuss, T.J., Wake, D.B., Zhang, Y.-P., 2010. Spiny frogs (Paini) illuminate the history of the Himalayan region and Southeast Asia. Proc. Natl. Acad. Sci. U. S. A. 107 (31), 13765–13770.
Christin, P.-A., Osborne, C.P., 2014. The evolutionary ecology of C4 plants. New Phytol. 204, 765–781.
Clift, P., Gaedicke, C., 2002. Accelerated mass flux to the Arabian Sea during the middle to late Miocene. Geology 30 (3), 207–210.
Clift, P.D., Hodges, K.V., Heslop, D., Hannigan, R., van Long, H., Calves, G., 2008. Correlation of Himalayan exhumation rates and Asian monsoon intensity. Nat. Geosci. 1, 875–880.
Corvinus, G., 1988. The Mio-Plio-Pleistocene litho- and bio- stratigraphy of the Surai Khola Siwaliks in west Nepal first results. CR Acad. Sci. Paris 306 (2), 1471–1477.
Corvinus, G., 1990. Litho- and biostratigraphy of the Siwalik succession in Surai Khola area, west Nepal. Palaeobotanist 38, 293–297.
Corvinus, G., 1993a. The Surai Khola Siwalik sequence in western Nepal (a contribution to the biostratigraphy of the Siwalik Group in Nepal). In: Jablonski, N. (Ed.), Evolving Landscapes and Evolving Biotas of East Asia since the Mid Tertiary. Centre of Asian Studies, Hong Kong, pp. 69–89.
Corvinus, G., 1993b. The Siwalik Group of sediments at Surai Khola in western Nepal and its paleontological record. J. Nep. Geol. Soc. 9, 21–35.
Corvinus, G., 1994. The Surai Khola and Rato Khola fossiliferous sequence in the Siwalik Group, Nepal. Himal. Geol. 15, 49–61.
Corvinus, G., Nanda, A.C., 1994. Stratigraphy and paleontology of the Siwalik Group of Surai Khola and Rato Khola in Nepal. N. Jb. Geol. Paläont. (Abh.) 191 (1), 25–68.
Corvinus, G., Rimal, L.N., 2001. Biostratigraphy and geology of the Neogene Siwalik

Group of the Surai Khola and Rato Khola areas in Nepal. Palaeogeogr. Palaeoclimatol. Palaeoecol. 165, 251–279.
Corvinus, G., Schleich, H., 1994. An Upper Siwalik reptile fauna from Nepal. Cour. Forschungsinst. Senck. 173, 239–259.
Dettman, D.L., Kohn, M.J., Quade, J., Ryerson, F.J., Ojha, T.P., Hamidullah, S., 2001. Seasonal stable isotope evidence for a strong Asian monsoon throughout the past 10.7 My. Geology 29, 31–34.
Dimri, A.P., Niyogi, D., Barros, A.P., Ridley, J., Mohanty, U.C., Yasunari, T., Sikka, D.R., 2015. Western disturbances: a review. Rev. Geophys. 53. http://dx.doi.org/10.1002/2014RG000460.
Ding, L., Spicer, R.A., Yang, J., Xu, Q., Cai, F., Li, S., Lai, Q., Wang, H., Spicer, T.E.V., Yue, Y., Shukla, A., Srivastava, G., Khan, M.A., Bera, S., Mehrotra, R., 2017. Quantifying the rise of the Himalaya orogen and implications for the South Asian Monsoon. Geology 45, 215–218.
Ferguson, D.K., 1985. The origin of leaf-assemblages: new light on an old problem. Rev. Palaeobot. Palynol. 46, 117–188.
Flynn, L.J., Jacobs, L.L., 1982. Effects of changing environments on Siwalik rodent faunas of northern Pakistan. Palaeogeogr. Palaeoclimatol. Palaeoecol. 38, 129–138.
Fox, D.L., Koch, P.L., 2003. Tertiary history of C4 biomass in the Great Plains, USA. Geology 31, 809–812.
Fox, D.L., Koch, P.L., 2004. Carbon and oxygen isotopic variability in Neogene paleosol carbonates: constraints on the evolution of the C4-grasslands of the Great Plains, USA. Palaeogeogr. Palaeoclimatol. Palaeoecol. 207, 305–329.
Gaut, B.S., Doebley, J.F., 1997. DNA sequence evidence for the segmental allotraploid origin of maize. Proc. Natl. Acad. Sci. U. S. A. 94, 6809–6814.
Guo, Z.T., Ruddiman, W.F., Hao, Q.Z., Wu, H.B., Qian, Y.S., Zhu, R.X., Peng, S.Z., Wei, J.J., Yuan, B.Y., Liu, T.S., 2002. Onset of Asian desertification by 22 Ma ago inferred from loess deposits in China. Nature 416, 159–163.
Gupta, A.K., Yuvaraja, A., Prakasama, M., Clemens, S.C., Velub, A., 2015. Evolution of the South Asian Monsoon wind system since the late Middle Miocene. Palaeogeogr. Palaeoclimatol. Palaeoecol. 438, 160–167.
Harrison, T.M., Copeland, P., Hall, S.A., Quade, J., Burner, S., Ojha, T.P., Kidd, W.S.F., 1993. Isotopic preservation of Himalayan–Tibetan uplift, denudation and climatic histories of two molasse deposits. J. Geol. 101, 157–175.
Hickey, L.J., 1977. Stratigraphy and paleobotany of the Golden Valley Formation (early tertiary) of western north Dakota. Geol. Soc. Am. Mem. 150, 1–183.
Hoorn, C., Ohja, T., Quade, J., 2000. Palynological evidence for vegetation development and climate change in the Sub-Himalayan Zone (Neogene, Central Nepal). Palaeogeogr. Palaeoclimatol. Palaeoecol. 163, 133–161.
Huang, Y.-J., Chen, Wen-Yun, Jacques, F.M.B., Liu, Yu-Sheng Christopher, Utescher, T., Su, T., Ferguson, D.K., Zhou, Zhe-Kun, 2015. Late Pliocene temperature and their spatial variation at the southeastern border of the Qinghai-Tibet Plateau. J. Asian Earth Sci. 111, 44–53.
Jacques, F.M.B., Guo, S.-X., Su, Tao, Xing, Yao-Wu, Huang, Yong-Jiang, Liu, Yu-Sheng Christopher, Ferguson, D.K., Zhou, Zhe-Kun, 2011. Quantitative reconstruction of the late Miocene monsoon climates of southwest China: a case study of the Lincang flora from Yunnan Province. Palaeogeogr. Palaeoclimatol. Palaeoecol. 304 (3–4), 318–327.
Kansakar, S.R., Hannah, D.M., Gerrard, J., Rees, G., 2004. Spatial pattern in the precipitation regime of Nepal. Int. J. Climatol. 24, 1645–1659.
Keeley, J.E., Rundel, P.W., 2005. Fire and the Miocene expansion of C4 grasslands. Ecol. Lett. 8, 683–690.
Khan, M.A., Spicer, R.A., Bera, S., Ghosh, R., Yang, J., Spicer, T.E.V., Guo, Shuang-Xing, Su, Tao, Jacques, F.M.B., Grote, P.J., 2014. Miocene to Pleistocene floras and climate of the eastern Himalayan Siwaliks, and new palaeoelevation estimates for the Namling-Oiyug Basin, Tibet. Glob. Planet. Chang. 113, 1–10.
Kingston, J.D., Marino, B.D., Hill, A., 1994. Isotopic evidence for Neogene hominid paleoenvironments in the Kenya Rift Valley. Science 264, 955–959.
Klaus, S., Morley, R.J., Plath, M., Zhang, Y.-P., Li, J.-T., 2015. Biotic interchange between the Indian subcontinent and mainland Asia through time. Nat. Commun. 7, 12132.
Knapp, A.K., Medina, E., 1999. Success of C4 photosynthesis in the field: lessons from communities dominated by C4 plants. In: Sage, R.F., Monson, R.K. (Eds.), C4 Plant Biology. Academic Press, NY, U.S.A., pp. 215–250.
Kroon, D., Steens, T., Troelstra, S.R., 1991. Onset of monsoonal related upwelling in the western Arabian Sea as revealed by planktonic foraminifers. In: Prell, W.L., Niitsuma, N. (Eds.), Proceedings of the Ocean Drilling Program, Scientific Results. vol. 117. Ocean Drilling Program, College Station, Texas, pp. 257–263.
Latorre, C., Quade, J., McIntosh, W.C., 1997. The expansion of C4 grasses and global climate change in the late Miocene: stable isotope evidence from the Americas. Earth Planet. Sci. Lett. 146, 83–96.
Li, Shu-Feng, Mao, Li-Mi, Spicer, R.A., Lebreton-Anberrée, J., Su, T., 2015. Late Miocene vegetation dynamics under monsoonal climate in southwestern China. Palaeogeogr. Palaeoclimatol. Palaeoecol. 425, 14–40.
Liang, M., Bruch, A., Collinson, M.E., Mosbrugger, V., Li, C.-S., Sun, Q., Hilton, J., 2003. Testing the climatic signals from different palaeobotanical methods: an example from the middle Miocene Shanwang flora of China. Palaeogeogr. Palaeoclimatol. Palaeoecol. 198, 279–301.
Liu, Yu-Sheng Christopher, Quan, C., 2016. Late Cenozoic climates of low-latitude East Asia: a paleobotanical example from the Baise basin of Guangxi, southern China. Palaeoworld 26, 572–580.
Liu, Yu-Sheng Christopher, Utescher, T., Zhou, Z.-K., Sun, B., 2011. The evolution of Miocene climates in North China: preliminary results of quantitative reconstructions from plant fossil records. Palaeogeogr. Palaeoclimatol. Palaeoecol. 304, 308–317.
Liu, Shuiyin, Zhu, Hua, Yang, Jie, 2017. A phylogenetic perspective on biogeographical divergence of the flora in Yunnan, southwestern China. Sci. Rep. 7, 43032.
Lundgren, M.R., Christin, P.A., Escobar, E.G., Ripley, B.S., Besnard, G., Long, C.M., Hattersley, P.W., Ellis, R.P., Leegood, R.C., Osborne, C.P., 2016. Evolutionary implications of C3–C4 intermediates in the grass *Alloteropsis semialata*. Plant Cell Environ. 39, 1874–1885.
MacGinitie, H.D., 1941. A middle Eocene flora from the central Sierra Nevada. Carnegie Inst. Wash. Publ. 534, 1–94 Washington.
Mehrotra, R.C., Liu, Xiu-Qun, Li, Cheng-Sen, Wang, Yu-Fei, Chauhan, M.S., 2005. Comparison of the Tertiary flora of southwest China and northeast India and its significance in the antiquity of the modern Himalayan flora. Rev. Palaeobot. Palynol. 135, 145–163.
Mehrotra, R.C., Shukla, A., Srivastava, G., Tiwari, R.P., 2014. Miocene megaflora of peninsular India: present status and future prospects. Spec. Pub. Palaeontol. Soc. India 5, 283–290.
Molnar, P., England, P., Martinod, J., 1993. Mantle dynamics, uplift of the Tibetan plateau, and the Indian monsoon. Rev. Geophys. 31, 357–396.
Molnar, P., Boos, W.R., Battisti, D.S., 2010. Orographic controls on climate and palaeoclimate of Asia: thermal and mechanical roles for the Tibetan Plateau. Annu. Rev. Earth Planet. Sci. 38, 77–102.
Mosbrugger, V., 1999. The nearest living relative method. In: Jones, T.P., Rowe, N.P. (Eds.), Fossil Plants and Spores Modern Techniques. Geol. Soc., London, pp. 261–265.
Mosbrugger, V., Utescher, T., 1997. The coexistence approach—a method for quantitative reconstructions of Tertiary terrestrial palaeoclimate data using plant fossils. Palaeogeogr. Palaeoclimatol. Palaeoecol. 134, 61–86.
Mosbrugger, V., Utescher, T., Dilcher, D.L., 2005. Cenozoic continental climatic evolution of Central Europe. Proc. Natl. Acad. Sci. U. S. A. 102, 14964–14969.
Nakayama, K., Ulak, P.D., 1999. Evolution of fluvial style in the Siwalik Group in the foothills of the Nepal Himalaya. Sediment. Geol. 125, 205–224.
Ojha, T.P., Butler, R.F., DeCelles, P.G., Quade, J., 2009. Magnetic polarity stratigraphy of the Neogene foreland basin deposits of Nepal. Basin Res. 21, 61–90.
Pausas, J.G., Ribeiro, E., 2017. Fire and plant diversity at the global scale. Glob. Ecol. Biogeogr. 26, 889–897.
Prasad, M., Awasthi, N., 1996. Contribution to the Siwalik flora of Surai Khola sequence, western Nepal and its palaeoecological and phytogeographical implications. Palaeobotanist 43, 1–42.
Prasad, M., Pandey, S.M., 2008. Plant diversity and climate during Siwalik (Miocene–Pliocene) in the Himalayan foothills of western Nepal. Palaeontogr. Abt. B 278, 13–70.
Prell, W.L., Murray, W.D., Clemens, S.C., Anderson, D.M., 1992. Evolution and variability of the Indian Ocean summer monsoon: evidence from the western Arabian Sea drilling program. In: Duncan, R.A., Rea, D.K., Kidd, R.B., von Rad, U., Weissel, J.K. (Eds.), Synthesis of Results from Scientific Drilling in the Indian Ocean, Geophysical Monograph. vol. 70. American Geophysical Union, Washington, DC, pp. 447–469.
Qin, F., Ferguson, D.K., Zetter, R., Wang, Y.F., Syabryaj, S., Li, J., Yang, J., Li, C.-S., 2011. Late Pliocene vegetation and climate of Zhangcun region, Shanxi, North China. Glob. Chang. Biol. 17, 1850–1870.
Quade, J., Cerling, T.E., Bowman, J.R., 1989. Development of Asian monsoon revealed by marked ecological shift during the latest Miocene in northern Pakistan. Nature 342, 163–166.
Quade, J., Solounias, N., Cerling, T.E., 1994. Stable isotopic evidence from paleosol carbonates and fossil teeth in Greece for forest or woodlands over the past 11 Ma. Palaeogeogr. Palaeoclimatol. Palaeoecol. 108, 41–53.
Quade, J., Cater, M.L.J., Ojha, P.T., Adam, J., Harrison, M.T., 1995. Late Miocene environmental change in Nepal and the northern Indian subcontinent: stable isotopic evidence from paleosols. GSA Bull. 107 (12), 1381–1397.
Quan, C., Liu, Yu-sheng Christopher, Utescher, T., 2011. Paleogene evolution of precipitation in northeastern China supporting the middle Eocene intensification of the east Asian monsoon. Palaios 26, 743–753.
Quan, C., Liu, Yu-sheng Christopher, Utescher, T., 2012. Eocene monsoon prevalence over China: a palaeobotanical perspective. Palaeogeogr. Palaeoclimatol. Palaeoecol. 365–366, 302–311.
Raymo, M.E., Ruddiman, W.F., 1992. Tectonic forcing of late Cenozoic climate. Nature 359, 117–122.
Rösler, W., Appel, E., 1998. Fidelity and time resolution of the magnetostratigraphic record in Siwalik sediments: high-resolution study of a complete polarity transition and evidence for cryptochrons in a Miocene fluviatile section. Geophys. J. Int. 135, 861–875.
Sage, R.F., 2004. The evolution of C4 photosynthesis. New Phytol. 161, 341–370.
Sanyal, P., Bhattacharya, S.K., Kumar, R., Ghosh, S.K., Sangode, S.J., 2004. Mio-Pliocene monsoonal record from Himalayan foreland basin (Indian Siwalik) and its relation to vegetational change. Palaeogeogr. Palaeoclimatol. Palaeoecol. 205, 23–41.
Sanyal, P., Bhattacharya, S.K., Prasad, M., 2005a. Chemical diagenesis of Siwalik sandstone: isotopic and mineralogical proxies from Surai Khola section, Nepal. Sediment. Geol. 180, 57–74.
Sanyal, P., Bhattacharya, S.K., Kumar, R., Ghosh, S.K., Sangode, S.J., 2005b. Palaeovegetational reconstruction in late Miocene: a case study based on early diagenetic carbonate cement from the Indian Siwalik. Palaeogeogr. Palaeoclimatol. Palaeoecol. 228, 245–259.
Sanyal, P., Sarkar, A., Bhattacharya, S.K., Kumar, R., Ghosh, S.K., Agrawal, S., 2010. Intensification of monsoon, microclimate and asynchronous C4 appearance: isotopic evidence from the Indian Siwalik sediments. Palaeogeogr. Palaeoclimatol. Palaeoecol. 296, 165–173.

Sarkar, S., 1990. Siwalik pollen succession from Suria Khola of western Nepal and its reflection on palaeoecology. In: Jain, K.P., Tiwari, R.S. (Eds.), Proceeding Symposium Vistas in Indian Palaeobotany. Palaeobotanist. 38. pp. 319–324.
Sati, S.P., Juyal, N., 2016. Recent forest fire in Uttarakhand. Curr. Sci. 111 (12), 1893.
Singh, S., Parkash, B., Awasthi, A.K., Kumar, S., 2011. Late Miocene record of palaeovegetation from the Siwalik palaeosols of the Ramnagar sub-basin. Curr. Sci. 100, 213–222.
Spicer, R.A., 1981. The sorting and deposition of allochthonous plant material in a modern environment at Silwood Lake, Silwood Park, Berkshire, England. U. S. Geol. Surv. Prof. Pap. 1143, 1–77.
Spicer, R.A., Wolfe, J.A., 1987. Plant taphonomy of late Holocene deposits in Trinity (Clair Engle) Lake, Northern California. Paleobiology 13, 227–245.
Spicer, R.A., Ahlberg, A., Herman, A.B., Hofmann, Christa-Charlotte, Raikevich, M., Valdes, P.J., Markwick, P.J., 2008. The Late Cretaceous continental interior of Siberia: a challenge for climate models. Earth Planet. Sci. Lett. 267, 228–235.
Srivastava, G., Mehrotra, R.C., 2010. Tertiary Flora of Northeast India vis-à-vis movement of the Indian plate. Mem. Geol. Soc. India 75, 123–130.
Srivastava, G., Mehrotra, R.C., Shukla, A., Tiwari, R.P., 2014. Miocene vegetation and climate in extra peninsular India: megafossil evidences. Spec. Pub. Palaeontol. Soc. India 5, 273–281.
Srivastava, G., Trivedi, A., Mehrotra, R.C., Paudayal, Khum N., Limaye, Ruta B., Kumaran, K.P.N., Yadav, S.K., 2016. Monsoon variability over Peninsular India during Late Pleistocene: signatures of vegetation shift recorded in terrestrial archive from the corridors of Western Ghats. Palaeogeogr. Palaeoclimatol. Palaeoecol. 443, 57–65.
Su, T., Jacques, F.M.B., Spicer, R.A., Liu, Y.-S., Huang, Y.-J., Xing, Y.-W., Zhou, Z.-K., 2013. Post-Pliocene establishment of the present monsoonal climate in SW China: evidence from the late Pliocene Longmen megaflora. Clim. Past 9, 1911–1920.
Taiz, L., Zeiger, E., 2002. Plant Physiology, 3rd Edition. Sinauer Associates, Sunderland.
Tanaka, S., 1997. Uplift of the Himalaya and climatic change at 10 Ma—evidence from records of carbon stable isotopes and fluvial sediments in the Churia Group, central Nepal. J. Geol. Soc. Japan 103 (3), 253–264.
Tipple, B.J., Pagani, M., 2007. The Early origins of terrestrial C4 photosynthesis. Annu. Rev. Earth Planet. Sci. 35, 435–461.
Uhl, D., Klotz, S., Traiser, C., Thiel, C., Utescher, T., Kowalski, E., Dilcher, D.L., 2007. Cenozoic paleotemperatures and leaf physiognomy—a European perspective. Palaeogeogr. Palaeoclimatol. Palaeoecol. 248, 24–31.
Utescher, T., Mosbrugger, V., 2015. The Palaeoflora database. www.palaeoflora.de.
Utescher, T., Bruch, A.A., Erdei, B., François, L., Ivanov, D., Jacques, F.M.B., Kern, A.K., Liu, Y.-S.C., Mosbrugger, V., Spicer, R.A., 2014. The Coexistence Approach–Theoretical background and practical considerations of using plant fossils for climate quantification. Palaeogeogr. Palaeoclimatol. Palaeoecol. 410, 58–73.
Utescher, T., Bondarenk, O.V., Mosbrugger, V., 2015. The Cenozoic cooling–continental signals from the Atlantic and Pacific side of Eurasia. Earth Planet. Sci. Lett. 415, 121–133.
Valdiya, K.S., 2002. Emergence and evolution of Himalaya: reconstructing history in the light of recent studies. Prog. Phys. Geogr. 26 (3), 360–399.
Vögeli, N., Najman, Y., van der Beek, Peter, Huyghe, P., Wynn, Peter M., Govin, G., van der Veen, Iris, Sachse, D., 2017. Lateral variations in vegetation in the Himalaya since the Miocene and implications for climate evolution. Earth Planet. Sci. Lett. 471, 1–9.
Wang, Li, Schneider, H., Zhang, X.-C., Xiang, Q.-P., 2012. The rise of the Himalaya enforced the diversification of SE Asian ferns by altering the monsoon regimes. BMC Plant Biol. 12, 210.
Wang, Q., Spicer, R.A., Yang, J., Wang, Y.-F., Li, C.-S., 2013. The Eocene climate of China, the early elevation of the Tibetan Plateau and the onset of the Asian monsoon. Glob. Chang. Biol. 19, 3709–3728.
Wang, P.X., Wang, B., Cheng, H., Fasullo, J., Guo, Z.T., Kiefer, T., Liu, Z.Y., 2014. The global monsoon across timescales: coherent variability of regional monsoons. Clim. Past 10, 2007–2052.
Wedin, D.A., 2004. C4 grasses: resource use, ecology, and global change. In: Moser, L.E., Burson, B.L., Sollenberger, L.E. (Eds.), Warm-season C4 Grasses. ASA-CSSA-SSSA Monograph, Madison, WI, pp. 15–50.
Wu, H., Guo, Z.T., Guiot, J., Hatté, C., Peng, C., Yu, Y., Ge, J., Li, Q., Sun, A., Zhao, D., 2014. Elevation-induced climate change as a dominant factor causing the late Miocene C4 plant expansion in the Himalayan foreland. Glob. Chang. Biol. 20, 1461–1472.
Xia, Ke, Tao, S., Liu, Yu-Sheng Christopher, Xing, Yao-Wu, Jacques, F.M.B., Zhou, Z.K., 2009. Quantitative climate reconstructions of the late Miocene Xiaolongtan megaflora from Yunnan, southwest China. Palaeogeogr. Palaeoclimatol. Palaeoecol. 276, 80–86.
Xing, Y.W., Utescher, T., Jacques, F.M.B., Tao, S., Liu, Y.S., Huang, Y.J., Zhou, Z.K., 2012. Palaeoclimatic estimation reveals a weak winter monsoon in southwestern China during the late Miocene: evidence from plant macrofossils. Palaeogeogr. Palaeoclimatol. Palaeoecol. 358-360, 19–26.
Yao, Yi-Feng, Bruch, A.A., Mosbrugger, V., Li, Cheng-Sen, 2011. Quantitative reconstruction of Miocene climate patterns and evolution in southern China based on plant fossils. Palaeogeogr. Palaeoclimatol. Palaeoecol. 304, 291–307.
Zaleha, M.J., 1997. Siwalik paleosols (Miocene, northern Pakistan): genesis and controls on their formation. J. Sediment. Res. 67, 821–839.
Zhang, R., Jiang, D., Zhang, Z., Yu, E., 2015. The impact of regional uplift of the Tibetan Plateau on the Asian monsoon climate. Palaeogeogr. Palaeoclimatol. Palaeoecol. 417, 137–150.
Zhao, J.-L., Xia, Y.-M., Cannon, C.H., Kress, W.J., Li, Q.-J., 2016. Evolutionary diversification of alpine ginger reflects the early uplift of the Himalayan–Tibetan Plateau and rapid extrusion of Indochina. Gondwana Res. 32, 232–241.